31st Annual International Conference of the IEEE EMBS
Minneapolis, Minnesota, USA, September 2-6, 2009

Automated Beat Onset and Peak Detection Algorithm for Field-Collected Photoplethysmograms

Liangyou Chen, Andrew T. Reisner, and Jaques Reifman

Abstract—**Recent reports suggest that photoplethysmography (PPG), which is a component of routine pulse oximetry, may be useful for detecting hypovolemia. An essential step in extracting and analyzing common PPG features is the robust identification of onset and peak locations of the vascular beats, despite varying beat morphologies and major oscillations in the baseline. Some prior reports used manual analysis of the PPG waveform; however, for systematic widespread use, an automated method is required. In this paper, we report an algorithm that automatically detects beat onsets and peaks from noisy field-collected PPG waveforms. We validated the algorithm by clinician evaluation of 100 randomly selected PPG waveform samples. For 99% of the beats, the algorithm was able to credibly identify the onsets and peaks of vascular beats, although the precise locations were ambiguous, given the very noisy data from actual clinical operations. The algorithm appears promising, and future consideration of its diagnostic capabilities and limitations is warranted.**

I. Introduction

Recently, it has been suggested that photoplethysmography (PPG), which is a component of routine pulse oximetry, may be useful for detecting hypovolemia [1-3]. This prospect is attractive because PPG is an entirely non-invasive measurement that is nearly ubiquitous throughout a wide spectrum of clinical arenas where routine vital signs are measured. What has been observed is that exaggerated PPG pulse variability (in terms of amplitude and baseline oscillation) due to respiration is associated with hypovolemic states [1, 2]. This effect is analogous to pulsus paradoxus, which is a similar variability of arterial blood pressure.

However, despite the widespread use of PPG monitoring for hospitalized patients, published evidence supporting the clinical utility of PPG in hemorrhage detection is limited. One factor may be that, while these PPG measurements are relatively easy to obtain in a clinical arena, there are insufficient data analysis tools for efficiently processing the biomedical data. For instance, in one report, Shamir *et al.* [2] relied on hand measurements of paper recordings of the PPG waveform. Golparvar *et al.* [3] videotaped the PPG waveform and then measured the investigational PPG features in units of pixels of a video display. The Masimo SET pulse oximeter [4] does automatically output its own "perfusion index," defined as a ratio of the measured PPG pulsatile amplitude to its DC component, but this is essentially a "black-box" tool because, for an individual research subject, the actual data processing can be neither examined nor evaluated by the investigator. As a result, such a black-box tool may be suboptimal for some kinds of academic research in which a basic understanding of the underlying phenomenon is sought.

In this paper, we report a non-proprietary method for PPG-waveform analysis. In some ways, this signal-processing problem is analogous to electrocardiogram beat detection, e.g., R-wave detection algorithms. However, the morphology of the PPG, in which each beat is more rounded and less distinct than a QRS complex, raises unique considerations. The PPG waveform also has a tendency to exhibit notable "random" baseline oscillation. Therefore, beat detection of the PPG waveform is also different from beat detection of a continuous arterial blood pressure waveform (e.g., Zong *et al.* [5]); the latter is typically measured only in intensive care units and thus is much less prone to such "random" baseline oscillation.

II. Methods

A. Trauma dataset

This study was based on vital-sign data collected from 898 prehospital trauma patients, measured in the field by Propaq 206EL transport monitors (Protocol Systems; Beaverton, OR), downloaded to an attached personal digital assistant, and ultimately stored in our database [6]. The PPG waveform was recorded at 91 Hz. We have previously developed algorithms to quantify the reliability of field-collected waveforms and vital signs [7, 8]. In this paper, we report an algorithm to locate beat onset and peak positions from the PPG waveforms.

B. Onset and peak identification algorithm

We identified beat onsets and peaks from PPG waveforms in four stages: (1) PPG preprocessing and outlier removal, which removed outlier and missing data points; (2) PPG waveform smoothing and baseline establishment, where we computed three auxiliary smoother waveforms; (3) peak

Manuscript received June 18, 2009. This work was supported in part by the Combat Casualty Care Research Area Directorate of the U.S. Army Medical Research and Materiel Command (USAMRMC), Fort Detrick, Maryland.

L. Chen is with the Bioinformatics Cell, Telemedicine and Advanced Technology Research Center (TATRC), USAMRMC, Fort Detrick, Maryland 21702 (e-mail: lchen@bioanalysis.org).

A. T. Reisner is with the Massachusetts General Hospital Department of Emergency Medicine, Boston, Massachusetts 02114 and with the Bioinformatics Cell, TATRC, USAMRMC, Fort Detrick, Maryland 21702 (e-mail: areisner@partners.org).

J. Reifman is a Senior Research Scientist and Director of the Bioinformatics Cell, TATRC, USAMRMC, ATTN: MCMR-TT, Bldg. 363 Miller Drive, Fort Detrick, Maryland 21702 (corresponding author; phone: 301-619-7915; fax: 301-619-1983; e-mail: jaques.reifman@us.army.mil).

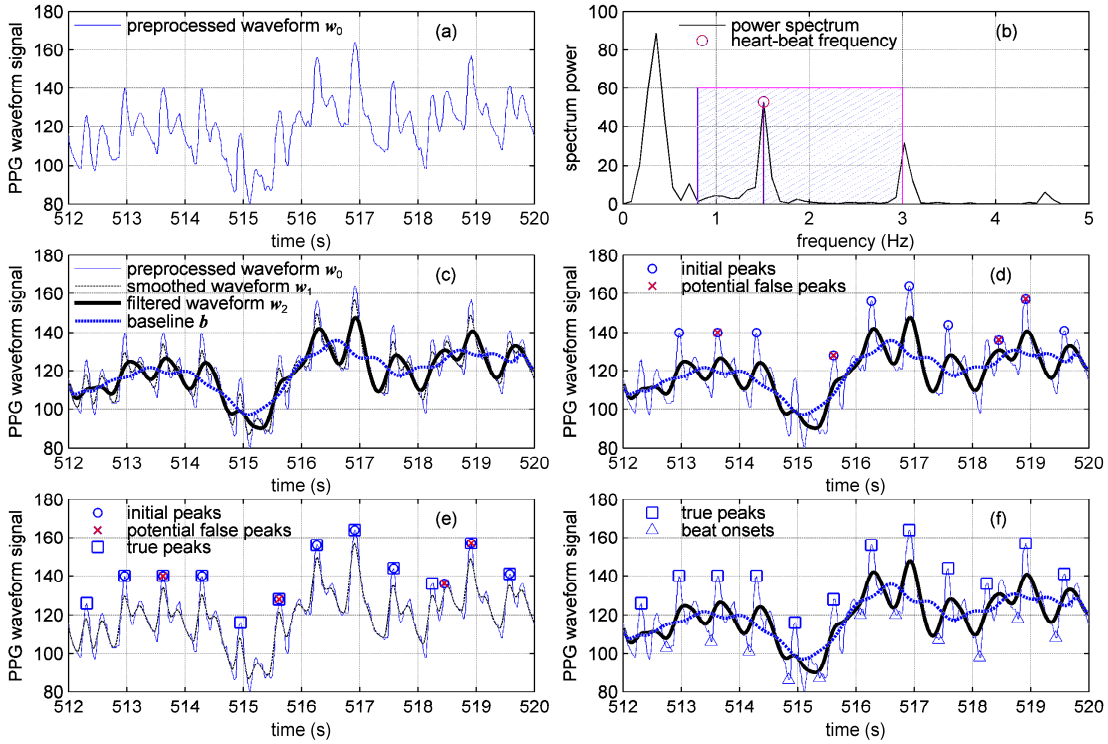

Fig. 1. Illustration of the onset and peak detection algorithm on an exemplary PPG waveform. Panel (a) shows the preprocessed waveform $\boldsymbol{w}_0$, which, in this case, is identical to the original waveform. Panel (b) shows the power spectrum density of $\boldsymbol{w}_0$ and that the frequency of the heartbeats is ~1.5 Hz. Panel (c) shows three additional auxiliary waveforms derived from $\boldsymbol{w}_0$. Panel (d) shows the initial peaks and potential false peaks identified by the algorithm. Panel (e) shows the locations of true peaks. Finally, Panel (f) shows the locations of beat onsets identified by the algorithm.

identification, where we detected true peaks; and (4) onset detection, where we identified beat onset locations. Fig. 1 together with the following description details the algorithm.

Stage 1. *PPG preprocessing and outlier removal*. We defined outliers of PPG waveforms as missing data points or data points with values >20 times the median waveform height. We linearly interpolated outlier data points that lasted for <0.2 s and used the resulting waveform, denoted as $\boldsymbol{w}_0$, as the starting signal for beat onset and peak detection. Fig. 1(a) illustrates an exemplary preprocessed PPG waveform $\boldsymbol{w}_0$ in our database. Since there are no outlier data points in this example, the original waveform is exactly the same as $\boldsymbol{w}_0$.

Stage 2. *PPG waveform smoothing and baseline establishment*. In this stage, we estimated the frequency of the heartbeats and computed three auxiliary waveforms with increasing smoothness: (i) a mildly smoothed waveform $\boldsymbol{w}_1$, which removed minor noise and sharp spikes; (ii) a low-pass-filtered waveform $\boldsymbol{w}_2$, which removed ectopic peaks; and (iii) a moving-average estimate of the waveform baseline $\boldsymbol{b}$ for peak detection.

We estimated the frequency of heartbeats in the input PPG waveform $\boldsymbol{w}_0$ by power spectrum analysis. Specifically, we linearly detrended $\boldsymbol{w}_0$ and computed its power spectrum density in the frequency domain using fast Fourier transform from MATLAB (Version 7.7). We estimated the frequency of the heartbeats as the frequency corresponding to the maximum power spectrum in the 0.8-3.0 Hz range (corresponding to normal heart rates from 50 to 180 beats/min) and estimated the average beat-to-beat interval as its reciprocal value. In Fig. 1(b), the frequency of the heartbeats is estimated to be ~1.5 Hz, with a corresponding beat-to-beat interval of 0.67 s. Based on this estimate, we computed the following three smoother waveforms:

i) *Mildly smoothed waveform* $\boldsymbol{w}_1$. We first smoothed the waveform $\boldsymbol{w}_0$ using a center median filter, with a window size set to one-fifth of the estimated beat-to-beat interval, followed by a center moving-average filter with the same window size. (The median filter was a robust filter but might introduce edge jitters. The moving-average filter reduced such edge jitters and enhanced the smoothness of the waveform signal.) The two filters removed noise and sharp spikes whose frequencies were more than five times that of the estimated heart-beat frequency. Fig. 1(c) illustrates that the smoothed waveform, denoted as $\boldsymbol{w}_1$, is smoother than $\boldsymbol{w}_0$ and has slightly lower amplitude at the peak positions.

ii) *Filtered waveform* $\boldsymbol{w}_2$. The smoothed waveform $\boldsymbol{w}_1$ was passed through a third-order, low-pass Butterworth filter with a cutoff frequency of one-and-a-half times the estimated heart-beat frequency. This filter removed ectopic peaks whose frequencies were higher than 1.5 the estimated heart-beat frequency. This filtered waveform is denoted as $\boldsymbol{w}_2$. Fig. 1(c) illustrates that two potential peaks on $\boldsymbol{w}_1$ between 517 and 518 s are filtered out, resulting in only one peak on $\boldsymbol{w}_2$ in this time interval.

iii) *Baseline* $\boldsymbol{b}$. We estimated a baseline $\boldsymbol{b}$ of the PPG waveform by applying a center moving-average filter to waveform $\boldsymbol{w}_2$, with a window size set to 1.5 of the estimated beat-to-beat interval. This selection attempted to optimize the

detection of PPG peaks at the heart-beat frequency [7] as discussed below in the onset and peak detection stages. Fig. 1(c) shows that baseline $\boldsymbol{b}$ is smoother than the filtered waveform $\boldsymbol{w}_2$ and reflects the baseline fluctuation of the PPG waveform.

Stage 3. *Peak identification*. We identified PPG peaks in three steps: (i) the identification of initial peaks, where we selected a set of initial peaks; (ii) the detection of potential false peaks, where we assessed the validity of each initial peak by analyzing the height of each peak and the peak-to-peak interval (to its preceding peak); and (iii) the relocation of potential missed peaks.

i) *Identification of initial peaks*. We identified an initial set of peaks on $\boldsymbol{w}_0$ by finding a local maximum in each time interval where the filtered waveform $\boldsymbol{w}_2$ is above the baseline $\boldsymbol{b}$ [Fig. 1(d)].

ii) *Detection of potential false peaks*. We detected potential false peaks from the initial set by imposing certain requirements on the peak's height and peak-to-peak interval. First, we sorted all peaks on $\boldsymbol{w}_0$ by height in increasing order and selected the height value at the 2/3 length position. Next, we required that each initial peak had a height greater than half of the selected height value. Then, we computed the median absolute deviation (MAD) of the peak-to-peak intervals $\boldsymbol{t}$, with MAD = median[|$\boldsymbol{t}$-median($\boldsymbol{t}$)|], and required that each interval not deviate from the median interval by more than two times MAD. We marked the PPG peaks not satisfying these two conditions as potential false peaks and the remaining as true peaks [Fig. 1(d)].

iii) *Relocation of missed peaks*. For intervals between true PPG peaks on $\boldsymbol{w}_0$ where potential false peaks were detected, we attempted to relocate putative false peaks and identify the locations of true ones. Specifically, starting from the left-boundary position of each interval, we advanced median($\boldsymbol{t}$) seconds and marked this point as the expected position of the next peak. Next, we searched around the expected position to identify a local maximum on the smoothed waveform $\boldsymbol{w}_1$ within a window size of length set to MAD. If the local maximum was located at either end of the window, we increased the window size by MAD seconds and repeated the process until the maximum was located inside the window. Then, we identified the equivalent maximum on $\boldsymbol{w}_0$ and labeled it as the next peak. Starting from this newly discovered peak position, we repeated the procedure above until we reached the end of the interval and by doing so recovered multiple consecutive missed peaks. We did not impose the peak height and peak-to-peak interval conditions described in the previous step on these newly discovered peaks and deemed them to be true peaks. Fig. 1(e) illustrates that a missed peak was recovered at 515 s, a potential false peak was confirmed to be a true peak between 515 and 516 s, and a false peak was relocated to an earlier time with a lower peak height between 518 and 519 s.

Stage 4. *Onset detection*. We identified the onset position corresponding to each true peak in three steps. First, we found ranges where $\boldsymbol{w}_0$ was below both the filtered waveform $\boldsymbol{w}_2$ and the baseline $\boldsymbol{b}$. This was to ensure that the identified onsets would be insensitive to different selections of baselines (here we considered the filtered waveform $\boldsymbol{w}_2$ as another potential baseline). Second, if there were multiple ranges identified, we ranked them based on their lengths, and selected the rightmost one from the top two ranges. This ensured that, when multiple potential onsets existed, we would find the major one closer to the left of the peak. Finally, we identified the minimum position on the waveform $\boldsymbol{w}_0$ in the selected range as the onset location. Fig. 1(f) illustrates the onsets identified by the algorithm.

C. Evaluation of the onset and peak detection algorithm

We validated the onset and peak detection algorithm by having an experienced clinician subjectively evaluate 30-s PPG waveform samples from 100 randomly selected subjects. We only included samples that were determined to be "reliable" according to our previously reported algorithm, which locates clean PPG waveform segments [8]. The clinician reviewed each identified beat, and sought to identify false beats, i.e., beats probably not due to a vascular pulsation, and missed beats.

III. Results

The 100 selected subjects had an average age of 39 yr (standard deviation 14 yr), including 72% male and 28% female, 13% prehospital intubated, 8% major hemorrhage, and 4% mortality rate. Except for a lower mortality rate (p=0.02) than the overall population of 898 patients (where the mortality rate was 10%), there were no statistically significant differences between this group and the overall population.

From the 100 sample waveforms, the algorithm identified 4605 peaks and 4505 onsets (the onset of the first peak was not identified in each segment). The human expert evaluated every peak and found 15 "probably bad" peaks, i.e., beats unlikely to be related to vascular pulsation, and zero missed peaks.

Fig. 2 shows typical onsets and peaks identified by the algorithm as well as the expert's evaluation of the questionable peaks (we show 15 s each due to limited space). Panel I shows two very clean PPG waveforms from which the algorithm correctly identified all peaks. Panel II shows some typical noisy waveforms with different morphologies, where the human expert determined that the algorithm had identified credible onsets and peaks. Finally, Panel III shows waveform samples where the expert identified one or more questionable peaks.

IV. Discussion and Conclusions

Our algorithm is able to adapt itself to different morphologies of PPG waveforms, detecting onsets and peaks from noisy waveforms that show substantial baseline instability. This automated algorithm may be useful for certain clinical investigations, which, in prior reports, required manual analysis of the PPG [2, 3]. The algorithm's

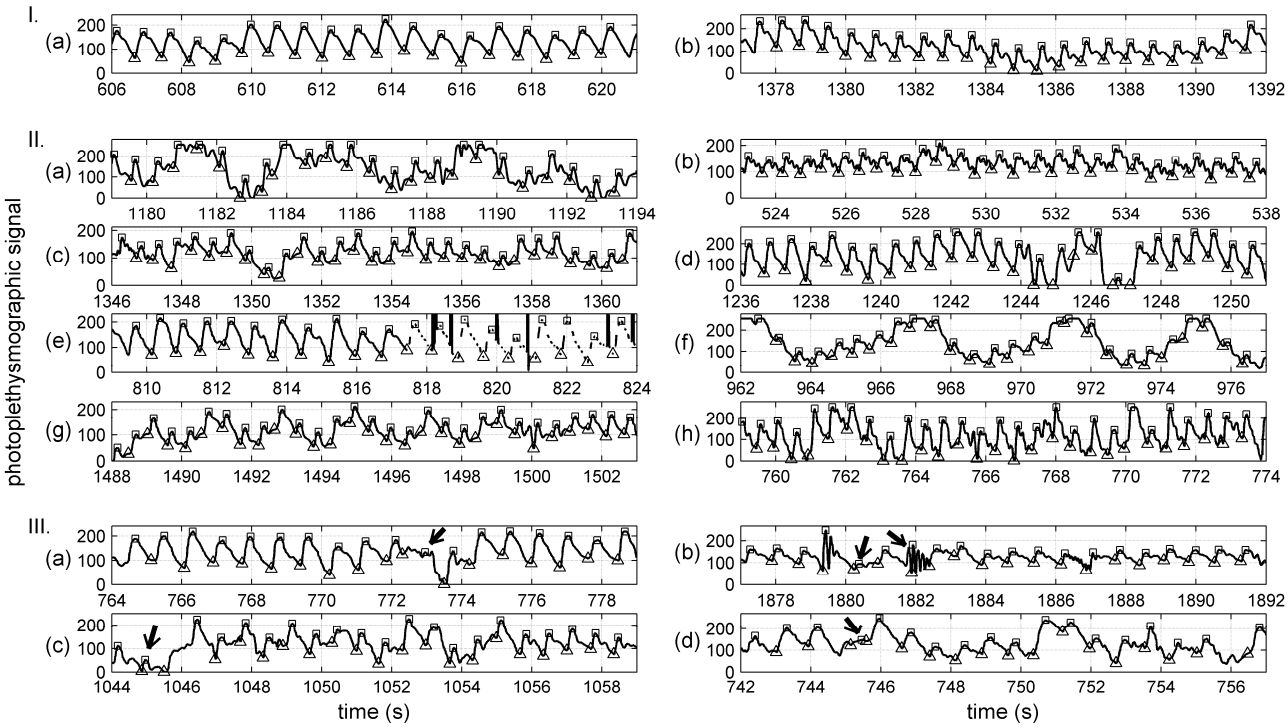

Fig. 2. Typical photoplethysmography (PPG) waveforms (black lines) from our database along with the detected peaks (rectangles) and detected onsets (triangles) identified by our algorithm. Panel I shows two very clean waveforms; Panel II shows eight noisy waveforms with varying morphologies, including missing (unconnected lines) and outlier data (vertical lines) in (e), where a human expert determined that the algorithm had identified credible onsets and peaks; and Panel III shows four noisy waveforms where the human expert considered five peaks as questionable (marked by arrows).

credible performance may be attributed to its use of multiple auxiliary waveforms with different levels of filtering, each of which accounted for different degrees of waveform variability. Its adaptive property may be particularly desirable for field use, where the morphology of the PPG waveform can change rapidly because of medic intervention or patient movement and the noisy nature of PPG measuring devices.

The major limitation of this report is the inherent challenge of validating noisy field data: given such waveforms from an uncontrolled prehospital environment, it is impossible to determine the precise "true" location of the beat onsets and peaks. This could, however, be resolved through simulations of clean signals with known superimposed noise. Also, we did not evaluate the diagnostic utility of our algorithm, i.e., whether it can yield superior information for the early diagnosis and prognosis of patient pathologies.

In our validation exercise, we found that, for the vast majority of cases, the algorithm's findings were credible, i.e., the identified beat onset and peak were "probably" due to a vascular pulsation. It was also apparent, though, that in many cases, these pulsations were quite distorted, even though the algorithm did a credible job of identifying the beat's onset and peak. In the future, it may or may not be advantageous to filter out excessively distorted beats from diagnostic consideration (or use additional waveform-cleaning methods to reduce the distortion). We are actively pursuing an evaluation of the diagnostic applications of the PPG waveform features, and evaluating whether there is diagnostic benefit to further filtering of excessively distorted beats.

DISCLAIMER

The opinions or assertions contained herein are the private views of the authors and are not to be construed as official or as reflecting the views of the U.S. Army or the U.S. Department of Defense.

REFERENCES

[1] A.P. Lima, P. Beelen, and J. Bakker, "Use of a peripheral perfusion index derived from the pulse oximetry signal as a noninvasive indicator of perfusion," *Crit Care Med*, vol. 30, (no. 6), pp. 1210-3, Jun 2002.

[2] M. Shamir, L.A. Eidelman, Y. Floman, L. Kaplan, and R. Pizov, "Pulse oximetry plethysmographic waveform during changes in blood volume," *Br J Anaesth*, vol. 82, (no. 2), pp. 178-81, Feb 1999.

[3] M. Golparvar, H. Naddafnia, and M. Saghaei, "Evaluating the relationship between arterial blood pressure changes and indices of pulse oximetric plethysmography," *Anesth Analg*, vol. 95, (no. 6), pp. 1686-90, Dec 2002.

[4] J.M. Goldman, M.T. Petterson, R.J. Kopotic, and S.J. Barker, "Masimo signal extraction pulse oximetry," *J Clin Monit Comput*, vol. 16, (no. 7), pp. 475-83, 2000.

[5] W. Zhong, T. Heldt, G.B. Moody, and R.G. Mark, "An open-source algorithm to detect onset of arterial blood pressure pulses," *Computers in Cardiology*, pp. 259- 262, Sep. 21-24 2003.

[6] T.M. McKenna, G. Bawa, K. Kumar, and J. Reifman, "The physiology analysis system: an integrated approach for warehousing, management and analysis of time-series physiology data," *Comput Methods Programs Biomed*, vol. 86, (no. 1), pp. 62-72, Apr 2007.

[7] L. Chen, T.M. McKenna, A.T. Reisner, and J. Reifman, "Algorithms to qualify respiratory data collected during the transport of trauma patients," *Physiol Meas*, vol. 27, (no. 9), pp. 797-816, Sep 2006.

[8] C. Yu, Z. Liu, T. McKenna, A.T. Reisner, and J. Reifman, "A method for automatic identification of reliable heart rates calculated from ECG and PPG waveforms," *J Am Med Inform Assoc*, vol. 13, (no. 3), pp. 309-20, May-Jun 2006.